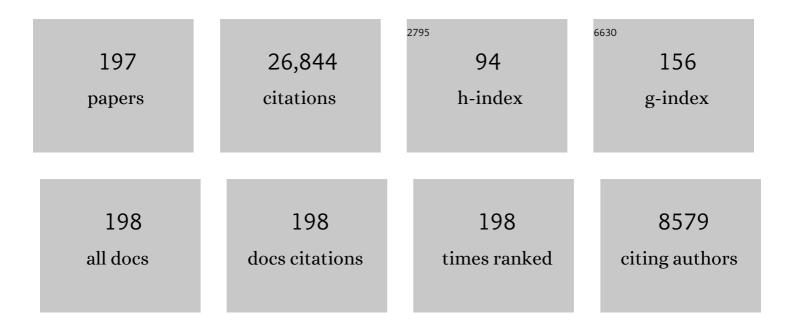
List of Publications by Year in descending order

Source: https://exaly.com/author-pdf/5184002/publications.pdf Version: 2024-02-01



WELCHEN

#	Article	IF	CITATIONS
1	Application of frequency ratio and weights of evidence models in landslide susceptibility mapping for the Shangzhou District of Shangluo City, China. Environmental Earth Sciences, 2016, 75, 1.	1.3	766
2	Application of fuzzy logic and analytical hierarchy process (AHP) to landslide susceptibility mapping at Haraz watershed, Iran. Natural Hazards, 2012, 63, 965-996.	1.6	758
3	A comparative study of logistic model tree, random forest, and classification and regression tree models for spatial prediction of landslide susceptibility. Catena, 2017, 151, 147-160.	2.2	637
4	Landslide susceptibility mapping using certainty factor, index of entropy and logistic regression models in GIS and their comparison at Mugling–Narayanghat road section in Nepal Himalaya. Natural Hazards, 2013, 65, 135-165.	1.6	559
5	Landslide susceptibility mapping using random forest, boosted regression tree, classification and regression tree, and general linear models and comparison of their performance at Wadi Tayyah Basin, Asir Region, Saudi Arabia. Landslides, 2016, 13, 839-856.	2.7	530
6	GIS-based groundwater potential mapping using boosted regression tree, classification and regression tree, and random forest machine learning models in Iran. Environmental Monitoring and Assessment, 2016, 188, 44.	1.3	489
7	Groundwater potential mapping at Kurdistan region of Iran using analytic hierarchy process and GIS. Arabian Journal of Geosciences, 2015, 8, 7059-7071.	0.6	417
8	Application of GIS-based data driven random forest and maximum entropy models for groundwater potential mapping: A case study at Mehran Region, Iran. Catena, 2016, 137, 360-372.	2.2	408
9	Landslide susceptibility mapping using index of entropy and conditional probability models in GIS: Safarood Basin, Iran. Catena, 2012, 97, 71-84.	2.2	400
10	Application of analytical hierarchy process, frequency ratio, and certainty factor models for groundwater potential mapping using GIS. Earth Science Informatics, 2015, 8, 867-883.	1.6	389
11	Landslide susceptibility mapping at Golestan Province, Iran: A comparison between frequency ratio, Dempster–Shafer, and weights-of-evidence models. Journal of Asian Earth Sciences, 2012, 61, 221-236.	1.0	378
12	Flood susceptibility mapping using frequency ratio and weights-of-evidence models in the Golastan Province, Iran. Geocarto International, 2016, 31, 42-70.	1.7	376
13	Landslide susceptibility mapping using J48 Decision Tree with AdaBoost, Bagging and Rotation Forest ensembles in the Guangchang area (China). Catena, 2018, 163, 399-413.	2.2	367
14	Application of frequency ratio, statistical index, and weights-of-evidence models and their comparison in landslide susceptibility mapping in Central Nepal Himalaya. Arabian Journal of Geosciences, 2014, 7, 725-742.	0.6	366
15	Performance evaluation of the GIS-based data mining techniques of best-first decision tree, random forest, and naÃ-ve Bayes tree for landslide susceptibility modeling. Science of the Total Environment, 2018, 644, 1006-1018.	3.9	341
16	Prediction of the landslide susceptibility: Which algorithm, which precision?. Catena, 2018, 162, 177-192.	2.2	338
17	A GIS-based flood susceptibility assessment and its mapping in Iran: a comparison between frequency ratio and weights-of-evidence bivariate statistical models with multi-criteria decision-making technique. Natural Hazards, 2016, 83, 947-987.	1.6	333
18	Landslide susceptibility assessment in Lianhua County (China): A comparison between a random forest data mining technique and bivariate and multivariate statistical models. Geomorphology, 2016, 259, 105-118.	1.1	330

#	Article	IF	CITATIONS
19	Flood susceptibility mapping using novel ensembles of adaptive neuro fuzzy inference system and metaheuristic algorithms. Science of the Total Environment, 2018, 615, 438-451.	3.9	330
20	Landslide susceptibility mapping at Vaz Watershed (Iran) using an artificial neural network model: a comparison between multilayer perceptron (MLP) and radial basic function (RBF) algorithms. Arabian Journal of Geosciences, 2013, 6, 2873-2888.	0.6	315
21	Flood susceptibility assessment in Hengfeng area coupling adaptive neuro-fuzzy inference system with genetic algorithm and differential evolution. Science of the Total Environment, 2018, 621, 1124-1141.	3.9	298
22	Landslide susceptibility modelling using GIS-based machine learning techniques for Chongren County, Jiangxi Province, China. Science of the Total Environment, 2018, 626, 1121-1135.	3.9	296
23	Landslide spatial modeling: Introducing new ensembles of ANN, MaxEnt, and SVM machine learning techniques. Geoderma, 2017, 305, 314-327.	2.3	280
24	Modeling flood susceptibility using data-driven approaches of naÃ ⁻ ve Bayes tree, alternating decision tree, and random forest methods. Science of the Total Environment, 2020, 701, 134979.	3.9	280
25	Application of fuzzy weight of evidence and data mining techniques in construction of flood susceptibility map of Poyang County, China. Science of the Total Environment, 2018, 625, 575-588.	3.9	279
26	Landslide susceptibility mapping using support vector machine and GIS at the Golestan Province, Iran. Journal of Earth System Science, 2013, 122, 349-369.	0.6	278
27	Landslide susceptibility assesssment in the Uttarakhand area (India) using GIS: a comparison study of prediction capability of naÃ̄ve bayes, multilayer perceptron neural networks, and functional trees methods. Theoretical and Applied Climatology, 2017, 128, 255-273.	1.3	264
28	Landslide susceptibility modeling applying machine learning methods: A case study from Longju in the Three Gorges Reservoir area, China. Computers and Geosciences, 2018, 112, 23-37.	2.0	262
29	Application of weights-of-evidence and certainty factor models and their comparison in landslide susceptibility mapping at Haraz watershed, Iran. Arabian Journal of Geosciences, 2013, 6, 2351-2365.	0.6	261
30	Groundwater qanat potential mapping using frequency ratio and Shannon's entropy models in the Moghan watershed, Iran. Earth Science Informatics, 2015, 8, 171-186.	1.6	259
31	Performance assessment of individual and ensemble data-mining techniques for gully erosion modeling. Science of the Total Environment, 2017, 609, 764-775.	3.9	258
32	Random forests and evidential belief function-based landslide susceptibility assessment in Western Mazandaran Province, Iran. Environmental Earth Sciences, 2016, 75, 1.	1.3	245
33	GIS-based groundwater potential analysis using novel ensemble weights-of-evidence with logistic regression and functional tree models. Science of the Total Environment, 2018, 634, 853-867.	3.9	245
34	GIS-based groundwater spring potential assessment and mapping in the Birjand Township, southern Khorasan Province, Iran. Hydrogeology Journal, 2014, 22, 643-662.	0.9	240
35	A Comparative Assessment Between Three Machine Learning Models and Their Performance Comparison by Bivariate and Multivariate Statistical Methods in Groundwater Potential Mapping. Water Resources Management, 2015, 29, 5217-5236.	1.9	213
36	Flood susceptibility modelling using novel hybrid approach of reduced-error pruning trees with bagging and random subspace ensembles. Journal of Hydrology, 2019, 575, 864-873.	2.3	213

#	Article	IF	CITATIONS
37	Applying population-based evolutionary algorithms and a neuro-fuzzy system for modeling landslide susceptibility. Catena, 2019, 172, 212-231.	2.2	210
38	GIS-based landslide susceptibility evaluation using a novel hybrid integration approach of bivariate statistical based random forest method. Catena, 2018, 164, 135-149.	2.2	207
39	Landslide susceptibility mapping using machine learning algorithms and comparison of their performance at Abha Basin, Asir Region, Saudi Arabia. Geoscience Frontiers, 2021, 12, 639-655.	4.3	206
40	Flash flood susceptibility analysis and its mapping using different bivariate models in Iran: a comparison between Shannon's entropy, statistical index, and weighting factor models. Environmental Monitoring and Assessment, 2016, 188, 656.	1.3	202
41	Gully erosion susceptibility assessment and management of hazard-prone areas in India using different machine learning algorithms. Science of the Total Environment, 2019, 668, 124-138.	3.9	202
42	Evaluation of different machine learning models for predicting and mapping the susceptibility of gully erosion. Geomorphology, 2017, 298, 118-137.	1.1	195
43	Gully erosion susceptibility mapping: the role of GIS-based bivariate statistical models and their comparison. Natural Hazards, 2016, 82, 1231-1258.	1.6	189
44	Spatial prediction of groundwater potential mapping based on convolutional neural network (CNN) and support vector regression (SVR). Journal of Hydrology, 2020, 588, 125033.	2.3	188
45	An integrated artificial neural network model for the landslide susceptibility assessment of Osado Island, Japan. Natural Hazards, 2015, 78, 1749-1776.	1.6	182
46	Landslide spatial modelling using novel bivariate statistical based NaÃ⁻ve Bayes, RBF Classifier, and RBF Network machine learning algorithms. Science of the Total Environment, 2019, 663, 1-15.	3.9	182
47	GIS-based landslide susceptibility modelling: a comparative assessment of kernel logistic regression, Naìve-Bayes tree, and alternating decision tree models. Geomatics, Natural Hazards and Risk, 2017, 8, 950-973.	2.0	179
48	Investigation of general indicators influencing on forest fire and its susceptibility modeling using different data mining techniques. Ecological Indicators, 2016, 64, 72-84.	2.6	178
49	GIS-based spatial prediction of flood prone areas using standalone frequency ratio, logistic regression, weight of evidence and their ensemble techniques. Geomatics, Natural Hazards and Risk, 2017, 8, 1538-1561.	2.0	178
50	New Hybrids of ANFIS with Several Optimization Algorithms for Flood Susceptibility Modeling. Water (Switzerland), 2018, 10, 1210.	1.2	174
51	GIS-based landslide susceptibility assessment using optimized hybrid machine learning methods. Catena, 2021, 196, 104833.	2.2	171
52	Flood susceptibility mapping in Dingnan County (China) using adaptive neuro-fuzzy inference system with biogeography based optimization and imperialistic competitive algorithm. Journal of Environmental Management, 2019, 247, 712-729.	3.8	169
53	Analysis and evaluation of landslide susceptibility: a review on articles published during 2005–2016 (periods of 2005–2012 and 2013–2016). Arabian Journal of Geosciences, 2018, 11, 1.	0.6	166
54	A novel hybrid artificial intelligence approach based on the rotation forest ensemble and naÃ ⁻ ve Bayes tree classifiers for a landslide susceptibility assessment in Langao County, China. Geomatics, Natural Hazards and Risk, 2017, 8, 1955-1977.	2.0	162

#	Article	IF	CITATIONS
55	A comparative study of landslide susceptibility maps produced using support vector machine with different kernel functions and entropy data mining models in China. Bulletin of Engineering Geology and the Environment, 2018, 77, 647-664.	1.6	161
56	Shallow Landslide Susceptibility Mapping: A Comparison between Logistic Model Tree, Logistic Regression, NaÃ⁻ve Bayes Tree, Artificial Neural Network, and Support Vector Machine Algorithms. International Journal of Environmental Research and Public Health, 2020, 17, 2749.	1.2	159
57	Spatial modelling of gully erosion in Mazandaran Province, northern Iran. Catena, 2018, 161, 1-13.	2.2	155
58	Evaluating the influence of geo-environmental factors on gully erosion in a semi-arid region of Iran: An integrated framework. Science of the Total Environment, 2017, 579, 913-927.	3.9	152
59	Assessment of the importance of gully erosion effective factors using Boruta algorithm and its spatial modeling and mapping using three machine learning algorithms. Geoderma, 2019, 340, 55-69.	2.3	152
60	Spatial prediction of groundwater potentiality using ANFIS ensembled with teaching-learning-based and biogeography-based optimization. Journal of Hydrology, 2019, 572, 435-448.	2.3	150
61	GIS-based multivariate adaptive regression spline and random forest models for groundwater potential mapping in Iran. Environmental Earth Sciences, 2016, 75, 1.	1.3	149
62	Novel GIS Based Machine Learning Algorithms for Shallow Landslide Susceptibility Mapping. Sensors, 2018, 18, 3777.	2.1	146
63	A GIS-based comparative study of Dempster-Shafer, logistic regression and artificial neural network models for landslide susceptibility mapping. Geocarto International, 2017, 32, 367-385.	1.7	143
64	GIS-based evaluation of landslide susceptibility using hybrid computational intelligence models. Catena, 2020, 195, 104777.	2.2	143
65	Landslide Susceptibility Modeling Based on GIS and Novel Bagging-Based Kernel Logistic Regression. Applied Sciences (Switzerland), 2018, 8, 2540.	1.3	140
66	Assessment of a data-driven evidential belief function model and GIS for groundwater potential mapping in the Koohrang Watershed, Iran. Geocarto International, 2015, 30, 662-685.	1.7	139
67	Applying Information Theory and GIS-based quantitative methods to produce landslide susceptibility maps in Nancheng County, China. Landslides, 2017, 14, 1091-1111.	2.7	136
68	Novel hybrid artificial intelligence approach of bivariate statistical-methods-based kernel logistic regression classifier for landslide susceptibility modeling. Bulletin of Engineering Geology and the Environment, 2019, 78, 4397-4419.	1.6	135
69	Landslide susceptibility modeling based on ANFIS with teaching-learning-based optimization and Satin bowerbird optimizer. Geoscience Frontiers, 2021, 12, 93-107.	4.3	133
70	Landslide susceptibility modeling in a landslide prone area in Mazandarn Province, north of Iran: a comparison between GLM, GAM, MARS, and M-AHP methods. Theoretical and Applied Climatology, 2017, 130, 609-633.	1.3	129
71	Spatial Prediction of Landslide Susceptibility Using GIS-Based Data Mining Techniques of ANFIS with Whale Optimization Algorithm (WOA) and Grey Wolf Optimizer (GWO). Applied Sciences (Switzerland), 2019, 9, 3755.	1.3	129
72	A comparison between ten advanced and soft computing models for groundwater qanat potential assessment in Iran using R and GIS. Theoretical and Applied Climatology, 2018, 131, 967-984.	1.3	127

#	Article	IF	CITATIONS
73	GIS-based gully erosion susceptibility mapping: a comparison among three data-driven models and AHP knowledge-based technique. Environmental Earth Sciences, 2018, 77, 1.	1.3	125
74	Novel Hybrid Evolutionary Algorithms for Spatial Prediction of Floods. Scientific Reports, 2018, 8, 15364.	1.6	124
75	Flood Spatial Modeling in Northern Iran Using Remote Sensing and GIS: A Comparison between Evidential Belief Functions and Its Ensemble with a Multivariate Logistic Regression Model. Remote Sensing, 2019, 11, 1589.	1.8	124
76	Landslide Susceptibility Modeling Using Integrated Ensemble Weights of Evidence with Logistic Regression and Random Forest Models. Applied Sciences (Switzerland), 2019, 9, 171.	1.3	124
77	GIS-based landslide spatial modeling in Ganzhou City, China. Arabian Journal of Geosciences, 2016, 9, 1.	0.6	123
78	Spatial prediction of landslide susceptibility using data mining-based kernel logistic regression, naive Bayes and RBFNetwork models for the Long County area (China). Bulletin of Engineering Geology and the Environment, 2019, 78, 247-266.	1.6	122
79	Landslide Detection and Susceptibility Mapping by AIRSAR Data Using Support Vector Machine and Index of Entropy Models in Cameron Highlands, Malaysia. Remote Sensing, 2018, 10, 1527.	1.8	121
80	Landslide Susceptibility Evaluation and Management Using Different Machine Learning Methods in The Gallicash River Watershed, Iran. Remote Sensing, 2020, 12, 475.	1.8	121
81	Land Subsidence Susceptibility Mapping in South Korea Using Machine Learning Algorithms. Sensors, 2018, 18, 2464.	2.1	120
82	Multi-hazard probability assessment and mapping in Iran. Science of the Total Environment, 2019, 692, 556-571.	3.9	119
83	Flood susceptibility mapping using geospatial frequency ratio technique: a case study of Subarnarekha River Basin, India. Modeling Earth Systems and Environment, 2018, 4, 395-408.	1.9	116
84	A hybrid fuzzy weight of evidence method in landslide susceptibility analysis on the Wuyuan area, China. Geomorphology, 2017, 290, 1-16.	1.1	115
85	Novel Hybrid Integration Approach of Bagging-Based Fisher's Linear Discriminant Function for Groundwater Potential Analysis. Natural Resources Research, 2019, 28, 1239-1258.	2.2	113
86	Spatial prediction of landslide susceptibility using hybrid support vector regression (SVR) and the adaptive neuro-fuzzy inference system (ANFIS) with various metaheuristic algorithms. Science of the Total Environment, 2020, 741, 139937.	3.9	113
87	Comparison of differences in resolution and sources of controlling factors for gully erosion susceptibility mapping. Geoderma, 2018, 330, 65-78.	2.3	111
88	Groundwater spring potential mapping using population-based evolutionary algorithms and data mining methods. Science of the Total Environment, 2019, 684, 31-49.	3.9	110
89	A Hybrid GIS Multi-Criteria Decision-Making Method for Flood Susceptibility Mapping at Shangyou, China. Remote Sensing, 2019, 11, 62.	1.8	110
90	GIS-based assessment of landslide susceptibility using certainty factor and index of entropy models for the Qianyang County of Baoji city, China. Journal of Earth System Science, 2015, 124, 1399-1415.	0.6	106

#	Article	IF	CITATIONS
91	Rainfall-induced landslide susceptibility assessment at the Chongren area (China) using frequency ratio, certainty factor, and index of entropy. Geocarto International, 0, , 1-16.	1.7	105
92	A novel hybrid integration model using support vector machines and random subspace for weather-triggered landslide susceptibility assessment in the Wuning area (China). Environmental Earth Sciences, 2017, 76, 1.	1.3	105
93	Spatial Modelling of Gully Erosion Using GIS and R Programing: A Comparison among Three Data Mining Algorithms. Applied Sciences (Switzerland), 2018, 8, 1369.	1.3	103
94	Forest fire susceptibility mapping in the Minudasht forests, Golestan province, Iran. Environmental Earth Sciences, 2015, 73, 1515-1533.	1.3	101
95	Comparison of four kernel functions used in support vector machines for landslide susceptibility mapping: a case study at Suichuan area (China). Geomatics, Natural Hazards and Risk, 2017, 8, 544-569.	2.0	100
96	GIS-based forest fire susceptibility mapping in Iran: a comparison between evidential belief function and binary logistic regression models. Scandinavian Journal of Forest Research, 2016, 31, 80-98.	0.5	99
97	Spatial prediction of landslide susceptibility by combining evidential belief function, logistic regression and logistic model tree. Geocarto International, 2019, 34, 1177-1201.	1.7	99
98	Prioritization of effective factors in the occurrence of land subsidence and its susceptibility mapping using an SVM model and their different kernel functions. Bulletin of Engineering Geology and the Environment, 2019, 78, 4017-4034.	1.6	99
99	Optimization of Computational Intelligence Models for Landslide Susceptibility Evaluation. Remote Sensing, 2020, 12, 2180.	1.8	99
100	Spatial modelling of gully erosion using evidential belief function, logistic regression, and a new ensemble of evidential belief function–logistic regression algorithm. Land Degradation and Development, 2018, 29, 4035-4049.	1.8	98
101	Evaluating the usage of tree-based ensemble methods in groundwater spring potential mapping. Journal of Hydrology, 2020, 583, 124602.	2.3	98
102	Comparison of machine learning models for gully erosion susceptibility mapping. Geoscience Frontiers, 2020, 11, 1609-1620.	4.3	96
103	Prioritization of landslide conditioning factors and its spatial modeling in Shangnan County, China using CIS-based data mining algorithms. Bulletin of Engineering Geology and the Environment, 2018, 77, 611-629.	1.6	94
104	Landslide susceptibility assessment at the Wuning area, China: a comparison between multi-criteria decision making, bivariate statistical and machine learning methods. Natural Hazards, 2019, 96, 173-212.	1.6	94
105	Spatial modeling, risk mapping, change detection, and outbreak trend analysis of coronavirus (COVID-19) in Iran (days between February 19 and June 14, 2020). International Journal of Infectious Diseases, 2020, 98, 90-108.	1.5	94
106	A novel ensemble approach of bivariate statistical-based logistic model tree classifier for landslide susceptibility assessment. Geocarto International, 2018, 33, 1398-1420.	1.7	93
107	Investigating the effects of different landslide positioning techniques, landslide partitioning approaches, and presence-absence balances on landslide susceptibility mapping. Catena, 2020, 187, 104364.	2.2	92
108	GIS-Based Machine Learning Algorithms for Gully Erosion Susceptibility Mapping in a Semi-Arid Region of Iran. Remote Sensing, 2020, 12, 2478.	1.8	92

#	Article	IF	CITATIONS
109	Landslide susceptibility mapping along Bhalubang — Shiwapur area of mid-Western Nepal using frequency ratio and conditional probability models. Journal of Mountain Science, 2014, 11, 1266-1285.	0.8	91
110	A comparative assessment between linear and quadratic discriminant analyses (LDA-QDA) with frequency ratio and weights-of-evidence models for forest fire susceptibility mapping in China. Arabian Journal of Geosciences, 2017, 10, 1.	0.6	91
111	Flash flood susceptibility modelling using functional tree and hybrid ensemble techniques. Journal of Hydrology, 2020, 587, 125007.	2.3	88
112	Shallow Landslide Susceptibility Mapping by Random Forest Base Classifier and Its Ensembles in a Semi-Arid Region of Iran. Forests, 2020, 11, 421.	0.9	87
113	A GIS-based comparative study of frequency ratio, statistical index and weights-of-evidence models in landslide susceptibility mapping. Arabian Journal of Geosciences, 2016, 9, 1.	0.6	84
114	GIS-based landslide susceptibility mapping using analytical hierarchy process (AHP) and certainty factor (CF) models for the Baozhong region of Baoji City, China. Environmental Earth Sciences, 2016, 75, 1.	1.3	84
115	PMT: New analytical framework for automated evaluation of geo-environmental modelling approaches. Science of the Total Environment, 2019, 664, 296-311.	3.9	84
116	Landslide Susceptibility Mapping Using Machine Learning Algorithms and Remote Sensing Data in a Tropical Environment. International Journal of Environmental Research and Public Health, 2020, 17, 4933.	1.2	84
117	Assessment of Landslide-Prone Areas and Their Zonation Using Logistic Regression, LogitBoost, and NaÃ ⁻ veBayes Machine-Learning Algorithms. Sustainability, 2018, 10, 3697.	1.6	82
118	Evaluation of different boosting ensemble machine learning models and novel deep learning and boosting framework for head-cut gully erosion susceptibility. Journal of Environmental Management, 2021, 284, 112015.	3.8	80
119	Gully headcut susceptibility modeling using functional trees, naÃ ⁻ ve Bayes tree, and random forest models. Geoderma, 2019, 342, 1-11.	2.3	79
120	Groundwater Spring Potential Mapping Using Artificial Intelligence Approach Based on Kernel Logistic Regression, Random Forest, and Alternating Decision Tree Models. Applied Sciences (Switzerland), 2020, 10, 425.	1.3	79
121	GIS-Based Gully Erosion Susceptibility Mapping: A Comparison of Computational Ensemble Data Mining Models. Applied Sciences (Switzerland), 2020, 10, 2039.	1.3	78
122	Landslide susceptibility mapping based on GIS and information value model for the Chencang District of Baoji, China. Arabian Journal of Geosciences, 2014, 7, 4499-4511.	0.6	76
123	A Comparative Assessment of Random Forest and k-Nearest Neighbor Classifiers for Gully Erosion Susceptibility Mapping. Water (Switzerland), 2019, 11, 2076.	1.2	75
124	GIS-Based Evaluation of Landslide Susceptibility Models Using Certainty Factors and Functional Trees-Based Ensemble Techniques. Applied Sciences (Switzerland), 2020, 10, 16.	1.3	75
125	Landslide Susceptibility Evaluation Using Hybrid Integration of Evidential Belief Function and Machine Learning Techniques. Water (Switzerland), 2020, 12, 113.	1.2	74
126	Uncertainty pattern in landslide susceptibility prediction modelling: Effects of different landslide boundaries and spatial shape expressions. Geoscience Frontiers, 2022, 13, 101317.	4.3	74

#	Article	IF	CITATIONS
127	Regional rainfall-induced landslide hazard warning based on landslide susceptibility mapping and a critical rainfall threshold. Geomorphology, 2022, 408, 108236.	1.1	73
128	Landslide susceptibility maps using different probabilistic and bivariate statistical models and comparison of their performance at Wadi Itwad Basin, Asir Region, Saudi Arabia. Bulletin of Engineering Geology and the Environment, 2016, 75, 63-87.	1.6	68
129	Hybrid Integration Approach of Entropy with Logistic Regression and Support Vector Machine for Landslide Susceptibility Modeling. Entropy, 2018, 20, 884.	1.1	67
130	Is multi-hazard mapping effective in assessing natural hazards and integrated watershed management?. Geoscience Frontiers, 2020, 11, 1203-1217.	4.3	67
131	A machine learning framework for multi-hazards modeling and mapping in a mountainous area. Scientific Reports, 2020, 10, 12144.	1.6	66
132	Application of frequency ratio, weights of evidence and evidential belief function models in landslide susceptibility mapping. Geocarto International, 0, , 1-21.	1.7	65
133	Landslide susceptibility mapping based on GIS and support vector machine models for the Qianyang County, China. Environmental Earth Sciences, 2016, 75, 1.	1.3	64
134	A Hybrid Computational Intelligence Approach to Groundwater Spring Potential Mapping. Water (Switzerland), 2019, 11, 2013.	1.2	64
135	Evaluation of multi-hazard map produced using MaxEnt machine learning technique. Scientific Reports, 2021, 11, 6496.	1.6	63
136	Novel Entropy and Rotation Forest-Based Credal Decision Tree Classifier for Landslide Susceptibility Modeling. Entropy, 2019, 21, 106.	1.1	61
137	Spatial modelling of gully headcuts using UAV data and four best-first decision classifier ensembles (BFTree, Bag-BFTree, RS-BFTree, and RF-BFTree). Geomorphology, 2019, 329, 184-193.	1.1	58
138	Combining Evolutionary Algorithms and Machine Learning Models in Landslide Susceptibility Assessments. Remote Sensing, 2020, 12, 3854.	1.8	58
139	Landslide Detection and Susceptibility Modeling on Cameron Highlands (Malaysia): A Comparison between Random Forest, Logistic Regression and Logistic Model Tree Algorithms. Forests, 2020, 11, 830.	0.9	57
140	Hybrid Computational Intelligence Methods for Landslide Susceptibility Mapping. Symmetry, 2020, 12, 325.	1.1	56
141	Evaluation efficiency of hybrid deep learning algorithms with neural network decision tree and boosting methods for predicting groundwater potential. Geocarto International, 2022, 37, 5564-5584.	1.7	54
142	Using machine learning algorithms to map the groundwater recharge potential zones. Journal of Environmental Management, 2020, 265, 110525.	3.8	52
143	Remote Sensing Data Derived Parameters and its Use in Landslide Susceptibility Assessment Using Shannon's Entropy and GIS. Applied Mechanics and Materials, 0, 225, 486-491.	0.2	51
144	Soil erosion assessment using RUSLE model and its validation by FR probability model. Geocarto International, 2020, 35, 1750-1768.	1.7	51

#	Article	IF	CITATIONS
145	An assessment of metaheuristic approaches for flood assessment. Journal of Hydrology, 2020, 582, 124536.	2.3	50
146	Applying different scenarios for landslide spatial modeling using computational intelligence methods. Environmental Earth Sciences, 2017, 76, 1.	1.3	49
147	Location-allocation modeling for emergency evacuation planning with GIS and remote sensing: A case study of Northeast Bangladesh. Geoscience Frontiers, 2021, 12, 101095.	4.3	49
148	Spatial Prediction of Landslides Using Hybrid Integration of Artificial Intelligence Algorithms with Frequency Ratio and Index of Entropy in Nanzheng County, China. Applied Sciences (Switzerland), 2020, 10, 29.	1.3	48
149	Groundwater recharge potential zonation using an ensemble of machine learning and bivariate statistical models. Scientific Reports, 2021, 11, 5587.	1.6	47
150	Application of frequency ratio, statistical index, and index of entropy models and their comparison in landslide susceptibility mapping for the Baozhong Region of Baoji, China. Arabian Journal of Geosciences, 2015, 8, 1829-1841.	0.6	46
151	Performance Evaluation of GIS-Based Artificial Intelligence Approaches for Landslide Susceptibility Modeling and Spatial Patterns Analysis. ISPRS International Journal of Geo-Information, 2020, 9, 443.	1.4	45
152	Spatial prediction of landslide susceptibility using integrated frequency ratio with entropy and support vector machines by different kernel functions. Environmental Earth Sciences, 2016, 75, 1.	1.3	43
153	SEVUCAS: A Novel GIS-Based Machine Learning Software for Seismic Vulnerability Assessment. Applied Sciences (Switzerland), 2019, 9, 3495.	1.3	42
154	Spatial Prediction of Landslide Susceptibility Based on GIS and Discriminant Functions. ISPRS International Journal of Geo-Information, 2020, 9, 144.	1.4	42
155	Modeling Spatial Flood using Novel Ensemble Artificial Intelligence Approaches in Northern Iran. Remote Sensing, 2020, 12, 3423.	1.8	41
156	Spatial prediction of rotational landslide using geographically weighted regression, logistic regression, and support vector machine models in Xing Guo area (China). Geomatics, Natural Hazards and Risk, 2017, 8, 1997-2022.	2.0	40
157	Landslide Susceptibility Mapping Using GIS-Based Data Mining Algorithms. Water (Switzerland), 2019, 11, 2292.	1.2	40
158	A comparative study on groundwater spring potential analysis based on statistical index, index of entropy and certainty factors models. Geocarto International, 2018, 33, 754-769.	1.7	39
159	Sedimentological characteristics and application of machine learning techniques for landslide susceptibility modelling along the highway corridor Nahan to Rajgarh (Himachal Pradesh), India. Catena, 2019, 182, 104150.	2.2	39
160	A Novel Intelligence Approach of a Sequential Minimal Optimization-Based Support Vector Machine for Landslide Susceptibility Mapping. Sustainability, 2019, 11, 6323.	1.6	37
161	Uncertainties Analysis of Collapse Susceptibility Prediction Based on Remote Sensing and GIS: Influences of Different Data-Based Models and Connections between Collapses and Environmental Factors. Remote Sensing, 2020, 12, 4134.	1.8	37
162	Evaluation of factors affecting gully headcut location using summary statistics and the maximum entropy model: Golestan Province, NE Iran. Science of the Total Environment, 2019, 677, 281-298.	3.9	36

#	Article	IF	CITATIONS
163	Toward the development of deep learning analyses for snow avalanche releases in mountain regions. Geocarto International, 2022, 37, 7855-7880.	1.7	36
164	Relations of land cover, topography, and climate to fire occurrence in natural regions of Iran: Applying new data mining techniques for modeling and mapping fire danger. Forest Ecology and Management, 2020, 473, 118338.	1.4	33
165	Hybrid Computational Intelligence Models for Improvement Gully Erosion Assessment. Remote Sensing, 2020, 12, 140.	1.8	33
166	Evaluation of Recent Advanced Soft Computing Techniques for Gully Erosion Susceptibility Mapping: A Comparative Study. Sensors, 2020, 20, 335.	2.1	33
167	Assessment of land degradation using machineâ€learning techniques: A case of declining rangelands. Land Degradation and Development, 2021, 32, 1452-1466.	1.8	33
168	Spatial Modeling of Gully Erosion Using Linear and Quadratic Discriminant Analyses in GIS and R. , 2019, , 299-321.		32
169	Groundwater spring potential assessment using new ensemble data mining techniques. Measurement: Journal of the International Measurement Confederation, 2020, 157, 107652.	2.5	32
170	Gully Head-Cut Distribution Modeling Using Machine Learning Methods—A Case Study of N.W. Iran. Water (Switzerland), 2020, 12, 16.	1.2	30
171	Comparison of new individual and hybrid machine learning algorithms for modeling and mapping fire hazard: a supplementary analysis of fire hazard in different counties of Golestan Province in Iran. Natural Hazards, 2020, 104, 305-327.	1.6	29
172	Incorporating Landslide Spatial Information and Correlated Features among Conditioning Factors for Landslide Susceptibility Mapping. Remote Sensing, 2021, 13, 2166.	1.8	29
173	A comparative study of statistical index and certainty factor models in landslide susceptibility mapping: a case study for the Shangzhou District, Shaanxi Province, China. Arabian Journal of Geosciences, 2015, 8, 9079-9088.	0.6	28
174	Deep learning and boosting framework for piping erosion susceptibility modeling: spatial evaluation of agricultural areas in the semi-arid region. Geocarto International, 2022, 37, 4628-4654.	1.7	27
175	Landslide susceptibility assessment and mapping using state-of-the art machine learning techniques. Natural Hazards, 2021, 108, 1291-1316.	1.6	27
176	Landslide susceptibility mapping using statistical bivariate models and their hybrid with normalized spatial-correlated scale index and weighted calibrated landslide potential model. Environmental Earth Sciences, 2021, 80, 1.	1.3	27
177	GISâ€based susceptibility assessment of the occurrence of gully headcuts and pipe collapses in a semiâ€arid environment: Golestan Province, NE Iran. Land Degradation and Development, 2019, 30, 2211-2225.	1.8	26
178	A new integrated data mining model to map spatial variation in the susceptibility of land to act as a source of aeolian dust. Environmental Science and Pollution Research, 2020, 27, 42022-42039.	2.7	26
179	Gully Erosion Susceptibility Mapping Using Multivariate Adaptive Regression Splines—Replications and Sample Size Scenarios. Water (Switzerland), 2019, 11, 2319.	1.2	25
180	Application of Fuzzy Analytical Network Process Model for Analyzing the Gully Erosion Susceptibility. Advances in Natural and Technological Hazards Research, 2019, , 105-125.	1.1	25

#	Article	IF	CITATIONS
181	Debris flows modeling using geo-environmental factors: developing hybridized deep-learning algorithms. Geocarto International, 2022, 37, 5150-5173.	1.7	24
182	Assessing, mapping, and optimizing the locations of sediment control check dams construction. Science of the Total Environment, 2020, 739, 139954.	3.9	20
183	Hybrids of Support Vector Regression with Grey Wolf Optimizer and Firefly Algorithm for Spatial Prediction of Landslide Susceptibility. Remote Sensing, 2021, 13, 4966.	1.8	16
184	Performance Evaluation and Comparison of Bivariate Statistical-Based Artificial Intelligence Algorithms for Spatial Prediction of Landslides. ISPRS International Journal of Geo-Information, 2020, 9, 696.	1.4	14
185	Gully head modelling in Iranian Loess Plateau under different scenarios. Catena, 2020, 194, 104769.	2.2	13
186	Volume, gravitational potential energy reduction, and regional centroid position change in the wake of landslides triggered by the 14 April 2010 Yushu earthquake of China. Arabian Journal of Geosciences, 2014, 7, 2129-2138.	0.6	12
187	Landslide susceptibility modeling based on remote sensing data and data mining techniques. Environmental Earth Sciences, 2022, 81, 1.	1.3	12
188	Comparing the Performance of a Logistic Regression and a Random Forest Model in Landslide Susceptibility Assessments. the Case of Wuyaun Area, China. , 2017, , 1043-1050.		10
189	Optimizing collapsed pipes mapping: Effects of DEM spatial resolution. Catena, 2020, 187, 104344.	2.2	10
190	Study on recognition of mine water sources based on statistical analysis. Arabian Journal of Geosciences, 2020, 13, 1.	0.6	9
191	Flash flood susceptibility mapping using stacking ensemble machine learning models. Geocarto International, 2024, 37, 15010-15036.	1.7	9
192	A novel hybrid bivariate statistical method entitled FROC for landslide susceptibility assessment. Environmental Earth Sciences, 2018, 77, 1.	1.3	8
193	Advanced machine learning algorithms for flood susceptibility modeling — performance comparison: Red Sea, Egypt. Environmental Science and Pollution Research, 2022, 29, 66768-66792.	2.7	8
194	A Review on the Gully Erosion and Land Degradation in Iran. Advances in Science, Technology and Innovation, 2020, , 393-403.	0.2	6
195	Comparison of statistical and machine learning approaches in land subsidence modelling. Geocarto International, 2022, 37, 6165-6185.	1.7	5
196	Gully Erosion Susceptibility Assessment Through the SVM Machine Learning Algorithm (SVM-MLA). Advances in Science, Technology and Innovation, 2020, , 415-425.	0.2	4
197	Landslide susceptibility modeling based on GIS and ensemble techniques. Arabian Journal of Geosciences, 2022, 15, 1.	0.6	4